Proteomics of the radioresistant phenotype in H1299 cells: SLC2A1 as a radiosensitivity marker

Xiaoling Xie (YF321901@163.com)
Lanzhou University First Affiliated Hospital
Yang Li
Lanzhou University
Zhiwu Liu
Lanzhou University
Yan Tang
Lanzhou University First Affiliated Hospital

Research

Keywords: Photon, H1299, proteomic, SLC2A1, iTRAQ

Posted Date: April 2nd, 2021

DOI: https://doi.org/10.21203/rs.3.rs-346547/v1

Abstract

Background: Radiotherapy is a main method for the treatment of malignant tumors. However, radiation resistance of tumor cells is the main reason for poor prognosis. The purpose of this study was to screen the differentially expressed protein (DEP), and its key protein related to radiation resistance in photon-resistant lung adenocarcinoma cell line H1299.

Methods: In this study, we investigated the cell viability and colony formation were examined to evaluate the potent proliferation-inhibiting effect of photo therapy on the H1299 cells. Flow cytometry was used to detect apoptosis. Further we selected the appropriate irradiation dose after photon irradiation of radioresistant cell H1299 for screening and validation of radioresistance-related DEPs by proteomic analysis. Furthermore, we also studied the SLC2A1 and irradiation sensitivity potential.

Results: The results showed a dose-dependent decrease of viable cell percentage following high dose of exposure (at dose of 8 and 10 Gy), and a prolonged the prolongation of H1299 cell cycle arrest, induced apoptosis. Proteomic analysis using iTRAQ revealed a total of 46 DEPs were identified including 30 up-regulated and 16 down-regulated DEPs in inhibition. Western blotting validated the respective changes in protein expression. DEPs were significantly associated with five-year survival in patients with lung adenocarcinoma. In addition, after knocking down SLC2A1, it was found that 4Gy radiation could significantly inhibit the proliferation of H1299 cells and regulate G2 phase arrest of cell cycle by down-regulating Cdk2.

Conclusions: These findings suggest the ITGA6,EIF4G1 and SLC2A1 protein is closely related to radiation resistance of lung adenocarcinoma, and SLC2A1 expression is significantly related to patient survival, so it can increase the sensitivity of H1299 cells to photon rays.

Introduction

In 2018, there were 18.1 million new cases of cancer worldwide, of which the incidence of lung cancer was 11.6% and the mortality rate was 18.4% [1] .The incidence of lung cancer has continued to increase worldwide, and lung cancer remains one of the most common causes of cancer-related death [2].Radiotherapy is an important treatment of lung cancer which could be applied as single treatment or combined with other therapeutic options in recent years [3]. In addition, some factors affect the sensitivity of lung cancer to radiotherapy, in which hypoxia theoretically inhibits the sensitivity to high single doses of radiation, meaning that hypoxic cells may improve resistance to radiotherapy[4]. A large number of studies have shown that the main factors of radiation resistance in tumor cells are endogenous radiation resistance, cell proliferation and oxygen deficiency. The data showed that the P53-deficient lung cancer cells H1299 are resistant to radiation enhancement[5]. While, these previous studies have been informative for many of the underlying mechanisms regulating cancer radioresistance. Therefore, elucidating the mechanisms and identifying novel biomarkers for radioresistance are urgently required and may provide key clues for the treatment of lung cancer.

The application of proteomic technologies has offered a precise mapping of genomic and proteomic alterations and the differential expression of key signaling proteins involved in tumor activation and progression. Using these approaches, we can now identify functional genes in many species using existing databases of proteins, such as UniProt and InterScan, through bioinformatics analysis, as well as Gene Ontology (GO) and Kyoto Encyclopedia of Gene and Genomes (KEGG) metabolic pathway analyses[6].We investigated the response of photon radiation to lung adenocarcinoma H1299 at the proteomic level, which provides insight into the relationship between radioresistance and lung adenocarcinoma protein molecules. HIF-1a, a transcription factor stabilized under hypoxia triggers the up-regulation of genes critical for the switch to glycolysis, including SLC2A1 (GLUT1), HKII, PDK1, PFK1, and lactate dehydrogenase LDHA [7, 8]. HIF proteins are important regulators of the tumorigenic capacity and therapy sensitivity of cancer cells; however, the regulatory mechanism of HIF-1 mediating the response of non-small cell like cancer (NSCLC) cells to radiation therapy needs further investigation. Cyclin-dependent kinase 2 (Cdk2) plays a pivotal part in cell cycle regulation and is involved in a range of biological processes. Cdk2 is a key cell cycle regulator, with roles in inactivating phosphorylation of the RB1 (pRb) tumour suppressor family and in controlling both G1/S and G2/M transitions[9]. Cdk2 has been described to play a positive role in cell cycle arrest in the DNA damage response (DDR), in particular at the G2/M checkpoint. Here we used proteomics and knockdown technologies to generate function reduction in SLC2A1 in H1299 NSCLC cells. Using these cells, we assessed the contribution of SLC2A1,Cdk2 and HIF-1 α factors as important mediators of radiation response and cell proliferation.

Methods

Cell culture and radiation conditions

Human lung adenocarcinoma H1299 cells were cultured with RPMI 1640 (Hyclon, USA) containing 10% FBS (Gibco, USA), penicillin (10 U/mL) and streptomycin (10 μg/mL) in a thermostatic incubator containing 5% CO2. Linear accelerator (Varian, USA) using single doses ranging between 4 and 10 Gy at 6 MV and a dose rate of 200 cGy/min for photon irradiation. The experiment was repeated three times.

Clonogenic survival and cell proliferation assay

The cells were inoculated into the culture flask to adjust the number of cells according to the dose (0 Gy:400, 4 Gy:800, 8 Gy:1600, 10 Gy:2000). After 14 days of irradiation, the formed cell colonies were fixed and stained, and the colonies of more than 50 cells were counted, and three independent experiments were carried out for each conditional sample. CCK-8 kit (Solarbio, Beijing, China) was used to detect the cell viability at 24, 48 and 72 hours after different doses of irradiation.

Cell cycle and apoptosis analysis

The irradiated cells culture was continued, and the cell cycle was detected at 48 h. Detection of cell cycle distribution labeled with propidium iodide (PI) by flow cytometry (BD, USA). The irradiated cells were collected and washed with pre-cooled PBS to make 1×10^6/ml cells suspension for flow cytometry to

detect apoptosis. The cells were stained with Annexin V and PI of 10 μl, then they were stained for 15 min without light, and then the binding buffer was added to detect the apoptosis rate by flow cytometry.

Protein isolation and iTRAQ labeling

Cells were collected and added 800 μl lysis buffer (50 mM Tris buffer, 8M Urea, 1% SDS, pH 8) containing complete protease inhibitor cocktail. Then they were lysed at 4°C for 30 min and centrifuged to collect and extract total proteins. Desalted peptides were labeled with iTRAQ reagents (iTRAQ® Reagent-8PLEX Multiplex Kit, Sigma), following the manufacturer's instructions (AB Sciex, Foster City, CA). For 0.1 mg of peptides,1 unit of labeling reagent was used.Therefore, Peptides were dissolved in 20 μl of 0.5 M triethylammonium bicarbonate solution (TEAB, pH 8.5), and the labeling reagent was added to 70 μl of isopropanol. After incubation for 1 h, the reaction was stopped with 50 mM Tris/HCl (pH 7.5). Differently labeled peptides were mixed equally and then desalted in 100 mg SCX columns.

LC-MS/MS analysis

Based on the MS/MS-HPLC online coupling mode of the obtained peptides after ionization and Q-Exactive by MS/MS method. Q-Exactive HF-X mass spectrometer was operated in positive polarity mode with capillary temperature of 320℃.Full MS scan resolution was set to 60000 with AGC target value of 3e6 for a scan range of 350-1500m/z. A data-dependent top 40 method was operated during witch HCD spectra was obtained at 15000 MS2 resolution with AGC target of 1e5 and maximum IT of 45 ms, 1.6 m/z isolation window, and NCE of 30, dynamically excluded of 60s.A data-dependent procedure that alternated between one MS scan followed by ten MS/MS scans that was applied for the ten most abundant precursor ions above a threshold ion count of 5000 in the MS survey scan[10].Gene Ontology (GO) and InterPro (IPR) analysis were conducted using the interproscan-5 program against the non-redundant protein database (including Pfam, PRINTS, ProDom, SMART, ProSiteProfiles, PANTHER) [11], and the databases COG (Clusters of Orthologous Groups) and KEGG (Kyoto Encyclopedia of Genes and Genomes) were used to analyze the protein family and pathway.

Western blot analysis and differential expression and survival correlation analysis in TCGA database

The cell lysate was mixed with SDS sample buffer and boiled in boiling water bath for 5 min, which can be detected and analyzed by SDS-PAGE electrophoresis. Through the protein was transferred onto a nitrocellulose membrane and incubation overnight at 4°C with the antibody against NRP1 (1: 2000) (Proteintech, #600671-Ig), ITGA6 (1: 1000) (Proteintech, #27189-1-AP), SLC2A1 (1: 1000) (Proteintech, #21829-1-AP), EIF4G1 (1: 10000) (Proteintech, #67199-1-Ig). After washing, the signals were detected with a HRP-conjugated secondary antibody (1: 5,000, Proteintech) for 1 h at RT, and visualized using an ECL chemiluminescent system, exposure was done using the Image Lab 3.0 system (Bio-Rad, USA). To further explore the correlation of NRP1, ITGA6, SLC2A1 and EIF4G1 expression levels with overall survival, we performed Kaplan-Meier analysis using TCGA database. The software R 3. 6. 0 was used for statistical analysis.

Transient Transfection

SLC2A1 expression plasmids was transiently transfected into H1299 cell lines by Lipofectamine 3000 (Invitrogen, Carlsbad, CA, USA), and the transfection protocol was conducted according to the manufacturer's instructions (Invitrogen, Carlsbad, CA, USA). human siSLC2A1 target sequence UGAUGUCCAGAAGAAUAGU, and siNC with target sequence CUUACGCUGAGUACUUCGA; Cell transfection was performed with Lipofectamine 3000 (Invitrogen) according to the manufacturer's instructions.

Reverse transcription PCR and quantitative PCR.

RNA was isolated using NucleoSpin RNA II kits (Clontech) and converted to cDNA using M-MLV Reverse Transcriptase (Invitrogen). Quantitative PCR (qPCR) was performed using ABI qPCR 7900HT (Thermo Fisher Scientific) by mixing cDNAs, Power SYBR Green PCR Master Mix (Invitrogen), and gene-specific primers. ACTB was used as internal control for normalization. Primer sequences are: SLC2A1-qF: CAGTTCGGCTATAACACCGGTGTC, SLC2A1-qR: GCCAAAGGGATTAACAAAGAGGCC; ACTB-qF: TCCCTGGAGAAGAGCTACGA, ACTB-qR: TACAGGTCTTTGCGGATGTC.

Statistical Analysis

All data are showed as mean ± standard deviation. One-way ANOVA was applied to determine the statistical differences followed by Dunnett's post-test (* $P < 0.05$).Proteins containing similar peptides and could not be distinguished based on MS/MS analysis were grouped separately as protein groups. Reporter Quantification (iTRAQ 8-plex) was used for iTRAQ quantification. The protein quantitation results were statistically analyzed by Mann-Whitney Test, the significant ratios, defined as $p < 0.05$ and $|\log 2\ FC| >$*(ratio > * or ratio < * [fold change, FC]), were used to screen the differentially expressed proteins (DEP).$P < 0.05$ was indicative of a statistically significant difference.

Results

Photons inhibit cell colony formation and proliferation

To evaluate the effects of X-ray irradiation on H1299cell viability, cells treated with different doses of either X-ray irradiation were assessed in terms of viable cell number using the plate count method. Exposure to 0–10 Gy of 6-MV X-ray irradiation resulted in the dose-dependent clonogenic survival of H1299 cells. Colony numbers of 8 Gy and 10 Gy irradiated H1299 cells was significantly greater than those 0 Gy ($P < 0.05$, Fig. 1A, 1B). The change was more pronounced in the high-dose (10 Gy) group. There is a correlation between time after radiation and cell viability (Fig. 1C), 48h after irradiation was chosen as the best time point for cell inhibition.

Photons induce apoptosis by arresting the cell cycle

To evaluate whether the cellular proliferation inhibition of H1299 cells in response to X-ray radiation is associated with apoptosis, H1299 cells were treated with X-ray radiation at 0, 4, 8 and 10 Gy. To achieve

significant cell death by x-ray irradiation in our in vitro model, we optimized the irradiation doses on H1299 cells by examining cell apoptosis after irradiation via FACS analysis. We find that the photons at high doses (4, 8, and 10 Gy) promoted S phase shortening of the H1299 cell cycle (Fig. 2A), cell cycle arrest at G2/M (Fig. 2B). Cell cycle arresting is one of the signals that can trig apoptosis. The results of apoptosis showed that compared with the control group (0 Gy), the apoptosis rate increased significantly at high dose of 8 and 10 Gy after irradiation (Fig. 2C, 2D) ($P < 0.05$).

Identification of DEPs and functional classification

Identification of DEPs between significant differences dose(8Gy) and control groups using an iTRAQ-based proteomic analysis. After 8 Gy of X-ray irradiation, the protein molecules in H1299 cells were subjected to data analysis, and the DEPs were obtained by clustering and bioinformatics analysis as shown in Fig. 3. A total of 2891 proteins were detected by iTRAQ-coupled 2D LC-MS/MS analysis. Among them, 191 proteins display significantly altered expression levels after irradiation. The representative distribution of up- and down-regulated proteins at 8 Gy after irradiation was showed in a volcano plot and heatmap compared to 0 Gy treated cells (Fig. 3A, B). The most 10 significantly differential proteins were listed in Table 1. KEGG pathway enrichment can be used to determine the signal transduction pathway of protein function, so as to obtain the prediction of protein possible function. These results showed that most DEPs were obviously enriched in the classifications of HIF-1α signaling pathway, TNF signaling pathway, choline metabolism as well as cell cycle pathway (Fig. 4C).

Table 1 List of proteins affected by X-ray and identified by LC/MS/MS

Accession	Gene Symbol	Ratio (24 hpi)	Coverage (95%)	Peptides (95%)	*p*-value	Function	Up.Down
NP_001019799.1	NRP1	1.253	48	12	0.02509003	Neuropilin-1	up
NP_004944.3	EIF4G1	1.025	18	6	0.004472103	Eukaryotic translation initiation factor 4 gamma 1	down
NP_001073286.1	ITGA6	1.348	10	9	0.00225449	Integrin alpha-6	up
NP_079375.3	CTC1	0.529	8	4	0.017618456	CST complex subunit CTC1	down
NP_006507.2	SLC2A1	1.355	51	16	0.001327805	Solute carrier family 2, facilitated glucose transporter member 1	down
NP_006588.1	HSPA8	1.133	17	4	4.89E-03	Heat shock cognate 71 kDa protein	up
XP_005245518.1	INTS3	0.954	3	3	0.013360981	Integrator complex subunit 3	down
NP_620061.2	PGK2	0.315	12	4	0.001276812	Phosphoglycerate kinase 2	down
NP_005092.1	ISG15	1.234	29	3	6.37E-04	Ubiquitin-like protein ISG15	down
NP_001138884.1	NFE2L2	1.352	14	7	0.004756	Nuclear factor erythroid 2-related factor 2	up

Verification of DEPs and survival correlation analysis of TCGA database and radio-sensitivity

To further validate the DEPs identified via iTRAQ-based LC-MS/MS, each of selected proteins were performed for western blot analysis. As shown in Fig. 3D, NRP1 (130 kDa), ITGA6 (119 kDa), SLC2A1 (54 kDa), EIF4G1 (175 kDa) and β-actin (42 kDa) were validated by western blot, which yielded the expected specific bands. Among which, two of the representative proteins (NRP1 and ITGA6) were up-regulated and two proteins (EIF4G1 and SLC2A1) were down-regulated after treatment with 8 Gy photon radiation in H1299 cells at 48 h. These findings were in agreement with the proteomic profiling. Proteomic levels of DEPs were positively correlated with their translational levels during photon radiation, consistent with the iTRAQ labelled LC-MS/MS data. The Kaplan–Meier survival analysis of NSCLC patients from the TCGA database demonstrated an positive correlation between EIF4G1 and SLC2A1 expression and NSCLC patient survival. Moreover, analysis of the TCGA database revealed that SLC2A1 and EIF4G1, which were down-regulated in the four differentially expressed molecules, were significantly reduced in lung adenocarcinoma. And up-regulated NRP1 and ITGA6 did not change significantly in lung adenocarcinoma. In addition to NRP1 protein, the expression levels of other three proteins DEPs, IGTA6, EIF4G1 and SLC2A1 were significantly correlated with five-year survival of lung adenocarcinoma patients (Fig. 4).

Next, we assessed the impact of SLC2A1 deletion on cell proliferation following irradiation. Compared with the control group, no differences in cell proliferation were observed between *siNC* and X-ray group, while the proliferation was significantly ($P < 0.05$) reduced for *siSLC2A1* and combination *group* (Fig. 5). Furthermore, only small differences were seen in the proliferative capacity of X-ray in comparison with control cells. In *siSLC2A1* group, a small but significant ($P < 0.05$) growth delay was observed compared to controland *siNC* conditions ($P < 0.05$). Forty-eight hours after X-ray + SLC2A1 siRNA knockdown, there was 31 ± 1% H1299 cells growth reduction compared with treatment with control (Fig. 5).

Cell cycle analysis after knockdown SLC2A1

Flow cytometry was used to determine the effect on cell cycle distribution in irradiated cells knockdown *SLC2A1* (Fig. 6). By contrast, no significant differences were observed between the *siSLC2A1* group and the control group ($P > 0.05$) (Fig. 6A, B). *siSLC2A1* and combination group showed a significat delay in cell proliferation, which was supported by a significant reduction in the S and increment G2 population (Fig. 6C,E). The increase in percentage of cells in G2/M was accompanied by a significant ($P < 0.05$) decrease in cells in S phase. In addition, *siSLC2A1* and combination group, incubated under normal conditions for 48 h, showed an overall decrease in S phase and accumulation in the G2/M phase (Fig. 6F). However, when irradiation was performed under X-ray, no additional effects on cell cycle distribution were observed (Fig. 6D).

Western Blotting and Real Time Quantitative PCR

To identify the immediate effects of SLC2A1 on the distribution and activation of cell cycle, we examined the expression of Cdk2 and HIF-1 α, 48 h after radiation (Fig. 7). Western blotting confirmed the reduce of SLC2A1 proteins (Fig. 7A). We observed a prominent increase in *SLC2A1 mRNA* and protein following knockdown and combination in H1299 cells, but without changed transcriptional and translational levels

of SLC2A1 and Cdk2 or HIF-1a in *siNC* and X-ray group. Meanwhile, no significant differences were observed between the X-ray group and the control group ($P > 0.05$).The overall expression levels of SLC2A1 were decreased in all the knockout models in comparison with control group (Fig. 7B). Next, we determined the mRNA expression levels of the cell cycles regulated genes SLC2A1, Cdk2 and HIF-1 α. We observed that the induction of HIF-1a genes was no compromised in the knockdown of SLC2A1 proteins (Fig. 7B).While, the expression of HIF-1a in the combined group decreased significantly.

Discussion

In recent years, with the development of radiotherapy equipment and technology, radiotherapy has shown good clinical effect for many kinds of cancers. However, due to the heterogeneity and radioresistance of lung cancer, the treatment and prognosis of some lung cancers are poor. Studies have shown a correlation between radiosensitivity and immunity as well[12]. Therefore, the exploration of radiation pattern and dose is the key of current research in this field. These results demonstrated that 8 and 10 Gy photons could inhibit the colony formation of H1299 cells, inhibit the proliferation of H1299 cells, arrest the tumor cell cycle in G2/M phase, and induce cell apoptosis. Radiation therapy leads to the failure of proper repair after DNA damage in cells, leading to cell death and inhibition of cell proliferation by apoptosis and other means [13]. It is possible that the X-rays of 8 and 10 Gy caused the double-strand break of DNA, thus inhibiting the proliferation of tumor cells. Most tumor cells cause different degrees of DNA strand breaks in cells after lethal doses of irradiation, and double-strand breaks in DNA are more difficult to repair, thus more likely to cause apoptosis [14]. Cells sensitive to ionizing radiation undergo apoptotic effects at a rapid rate [15]. It may also allow tumor cells to escape apoptosis induced by certain factors.

The samples of irradiated H1299 cells were isolated and identified by LC-MS/MS technique. Bioinformatics analysis can identify DEPs. SLC2A1 is a major component of cellular energy metabolism and is closely related to the HIF1 signaling pathway, and EIF4G1 is an important part of protein translation and is closely related to tumorigenesis. These functions and associated metabolic pathways provided a basis for understanding how photon radiation resistance promoted lung adenocarcinoma cell proliferation. Hypoxic tumor cells are more resistant to radiation, which can lead to the failure of radiotherapy and chemotherapy in tumor patients [16]. Photon radiation up-regulated the expression of ITGA6 in H1299 cells. ITGA6 was abundantly present in the plasma membrane and was essential for tumor growth and metastasis [17, 18]. In addition, the expression of NRP1 was associated with radioresistance in A549 cells, and can play a radioresistant role by activating signaling pathways such as PI3K-Akt, VEGF and TGF-β[19, 20]. Our study suggested that photon radiation promoted NRP1 expression by 8 Gy at 48 h. Other research showed that EGF promoted tumor stemness expression and self-renewal by acting directly on CSCs through an autocrine loop of NRP1, and knockdown of NRP1 in normal epithelium prevented tumorigenesis [21]. Therefore, NRP1 plays an important role in the occurrence and development of tumors. It has been found that the translation initiation complex EIF4F also played an important role in tumorigenesis, growth and therapeutic resistance of prostate cancer [22, 23].

Glucose transporter 1 (SLC2A1) plays an important role in tumor glycolysis and is closely related to tumor healing [18]. Previous studies have reported that SLC2A1 is over-expressed in several types of cancer, such as breast and lung cancer. The expression level of GLUT1 correlates with that of HIF-1 α in many cancer types, including colorectal and ovarian cancers[7]. In the anaerobic glycolysis pathway, HIF-1α first activates SLCA1 transcription to increase glucose uptake in cells. High expression of SLC2A1 is an early marker of malignant transformation and can be used as an important basis for predicting tumor prognosis [18].Clinical studies have shown that SLC2A1 protein is not expressed in normal or benign lesions, whereas SLC2A1 1 is highly expressed in malignant tumor tissues[24]. Our study found that photons of 8Gy could significantly inhibit the proliferation of H1299 cells, and further proteomics showed that the expression of SLC2A1 protein was down-regulated.In the process of tumor proliferation, tumor tissues are in a relatively hypoxic state, and the expression under hypoxic microenvironment, increased expression of HIF-1α has the potential to promote the proliferation and angiogenesis of small cell lung cancer [25, 26]. Hypoxic cells upregulate the HIF pathway which is associated with radiation resistance in many types of cancer, including NSCLC [27]. In our study, irradiated molecules participate in HIF-1 α signaling pathway, which may be related to the radiation resistance of H1299 cells. Some studies have indicated that the expression level of SLC2A1 can be used as an important indicator to evaluate tumor hypoxia and glucose metabolism. In this study, the results in the transcriptional level indicated that SLC2A1 molecules in cells were affected by different radiation doses, and after 8 and 10 Gy irradiation, the relative expression levels of the SLC2A1 molecules was decreased. While, there was no significant change in the expression of SLC2A1and HIF-1 α in cells after 4Gy irradiation. It has been shown that there is a linear positive correlation between SLC2A1 and HIF-1α mRNA expression in NSCLC tissues [28, 29], which may be that hypoxic tissues in the tumor activate the expression of the transcription factor HIF-1, acting on the downstream targeting molecule SLC2A1 molecules to make glycolysis faster. Cdk2 is not required for Chk1 activation and G2 arrest by agents that induce double strand DNA breaks. Research shows that inhibition of Cdk2 by the DNA damage response promotes a timely implementation of the G2 cell cycle exit programmers [30]. Our study showed that after knockdown, the cell cycle increased in G2 phase and decreased in S phase. Furthermore, this change is more obvious after X-ray exposure to 4Gy. This may be a down-regulation of SLC2A1, which can increase the radio sensitivity to X-rays. Cdk2 inhibition apparently hinders the DDR, and sensitizes cells to ionizing radiation, inducing cell death [30]. To complement the energy requirement for rapid tumor growth, HIF-1α can promote SLC2A1 expression in tumor cells. Recently, it has been found that irradiation of primary tumors in mice can accelerate the invasion and metastasis of malignant tumors[31]. It was confirmed in animal studies that HIF-1 plays a role in promoting tumor growth [32]. In hypoxia, activated HIF-1 binds to the downstream target gene SLC2A1 and activates transcriptional expression, thereby maintaining the energy metabolism of cells to promote tumor proliferation.

Conclusions

Our work may have relevant implications concerning how radio resistances are currently used in the basic research. Our data suggest that knockdown SLC2A1 in combination with radiation might increase

radiation sensitivity. Importantly, the specific inhibition of SLC2A1 accounts for critical changes in the proliferation and cell cycle of H1299 cells, including an increase in G2/M phase which might result in a defect in using SLC2A1 as an energetic transfer.

Declarations

Authors' contributions

Conception and design: Xiaoling Xie and Yang Li. Administrative support: Xiaoling Xie.
Experiment operation: Zhiwu Liu1, Yan Tang.Data analysis and interpretation: Xiaoling Xie and Yang Li.
Manuscript writing: All authors.The authors read and approved the final manuscript.

Fund

This study was supported by Scientific Research Projects of Gansu Health Industry Funding No. gswsky2018-42 .

Availability of data and materials

All the data in this research are available from TCGA database

Declarations

Ethics approval and consent to participate

Not applicable.

Consent for publication

Not applicable.

Competing interests

The authors declare that they have no competing interests.

References

1. Bray F, Ferlay J, Soerjomataram I, Siegel RL, Torre LA, Jemal A. Global cancer statistics 2018: GLOBOCAN estimates of incidence and mortality worldwide for 36 cancers in 185 countries. CA Cancer J Clin. 2018;68(6):394–424.
2. Rahib L, Smith BD, Aizenberg R, Rosenzweig AB, Fleshman JM, Matrisian LM. Projecting cancer incidence and deaths to 2030: the unexpected burden of thyroid, liver, and pancreas cancers in the United States. Cancer Res. 2014;74(11):2913–21.

3. Saadeddin A. Radiotherapy for NSCLC: review of conventional and new treatment techniques. J Infect Public Health. 2012;5(Suppl 1):45–9.
4. Hu CJ, Iyer S, Sataur A, Covello KL, Chodosh LA, Simon MC. Differential regulation of the transcriptional activities of hypoxia-inducible factor 1 alpha (HIF-1alpha) and HIF-2alpha in stem cells. Mol Cell Biol. 2006;26(9):3514–26.
5. Liu N, Wang YA, Sun Y, Ecsedy J, Sun J, Li X, Wang P. Inhibition of Aurora A enhances radiosensitivity in selected lung cancer cell lines. Respir Res. 2019;20(1):230.
6. Yang S, Zhang J, Yan Y, Yang M, Li C, Li J, Zhong L, Gong Q, Yu H. Network Pharmacology-Based Strategy to Investigate the Pharmacologic Mechanisms of Atractylodes macrocephala Koidz. for the Treatment of Chronic Gastritis. Front Pharmacol. 2019;10:1629.
7. Moldogazieva NT, Mokhosoev IM, Terentiev AA. Metabolic Heterogeneity of Cancer Cells: An Interplay between HIF-1, GLUTs, and AMPK. Cancers (Basel). 2020;12(4):862.
8. Bhalla K, Jaber S, Nahid MN, Underwood K, Beheshti A, Landon A, Bhandary B, Bastian P, Evens AM, Haley J, et al. Role of hypoxia in Diffuse Large B-cell Lymphoma: Metabolic repression and selective translation of HK2 facilitates development of DLBCL. Sci Rep. 2018;8(1):744.
9. Bacevic K, Lossaint G, Achour TN, Georget V, Fisher D, Dulic V. Cdk2 strengthens the intra-S checkpoint and counteracts cell cycle exit induced by DNA damage. Sci Rep. 2017;7(1):13429.
10. Kay R, Barton C, Ratcliffe L, Matharoo-Ball B, Brown P, Roberts J, Teale P, Creaser C. Enrichment of low molecular weight serum proteins using acetonitrile precipitation for mass spectrometry based proteomic analysis. Rapid Commun Mass Spectrom. 2008;22(20):3255–60.
11. Jung J, Lee HK, Yi G. A novel method for functional annotation prediction based on combination of classification methods. ScientificWorldJournal. 2014;2014:542824.
12. Murphy S, Zweyer M, Mundegar RR, Swandulla D, Ohlendieck K. Proteomic serum biomarkers for neuromuscular diseases. Expert Rev Proteomics. 2018;15(3):277–91.
13. Qi J, Zhao P, Li F, Guo Y, Cui H, Liu A, Mao H, Zhao Y, Zhang X. Down-regulation of Rab17 promotes tumourigenic properties of hepatocellular carcinoma cells via Erk pathway. Int J Clin Exp Pathol. 2015;8(5):4963–71.
14. Ma Y, Xiu Z, Zhou Z, Huang B, Liu J, Wu X, Li S, Tang X. Cytochalasin H Inhibits Angiogenesis via the Suppression of HIF-1alpha Protein Accumulation and VEGF Expression through PI3K/AKT/P70S6K and ERK1/2 Signaling Pathways in Non-Small Cell Lung Cancer Cells. J Cancer. 2019;10(9):1997–2005.
15. Jorgensen TJ. Enhancing radiosensitivity: targeting the DNA repair pathways. Cancer Biol Ther. 2009;8(8):665–70.
16. Kang J, Kim E, Kim W, Seong KM, Youn H, Kim JW, Kim J, Youn B. Rhamnetin and cirsiliol induce radiosensitization and inhibition of epithelial-mesenchymal transition (EMT) by miR-34a-mediated suppression of Notch-1 expression in non-small cell lung cancer cell lines. J Biol Chem. 2013;288(38):27343–57.

17. Horsman MR, Overgaard J. The impact of hypoxia and its modification of the outcome of radiotherapy. J Radiat Res. 2016;57(Suppl 1):i90–8.
18. Berlth F, Monig SP, Schlosser HA, Maus M, Baltin CT, Urbanski A, Drebber U, Bollschweiler E, Holscher AH, Alakus H. Validation of 2-mm tissue microarray technology in gastric cancer. Agreement of 2-mm TMAs and full sections for Glut-1 and Hif-1 alpha. Anticancer Res. 2014;34(7):3313–20.
19. Velpula KK, Rehman AA, Chelluboina B, Dasari VR, Gondi CS, Rao JS, Veeravalli KK. Glioma stem cell invasion through regulation of the interconnected ERK, integrin alpha6 and N-cadherin signaling pathway. Cell Signal. 2012;24(11):2076–84.
20. Roos A, Ding Z, Loftus JC, Tran NL. Molecular and Microenvironmental Determinants of Glioma Stem-Like Cell Survival and Invasion. Front Oncol. 2017;7:120.
21. Dong JC, Gao H, Zuo SY, Zhang HQ, Zhao G, Sun SL, Han HL, Jin LL, Shao LH, Wei W, et al. Neuropilin 1 expression correlates with the Radio-resistance of human non-small-cell lung cancer cells. J Cell Mol Med. 2015;19(9):2286–95.
22. Beck B, Driessens G, Goossens S, Youssef KK, Kuchnio A, Caauwe A, Sotiropoulou PA, Loges S, Lapouge G, Candi A, et al. A vascular niche and a VEGF-Nrp1 loop regulate the initiation and stemness of skin tumours. Nature. 2011;478(7369):399–403.
23. Sridharan S, Robeson M, Bastihalli-Tukaramrao D, Howard CM, Subramaniyan B, Tilley AMC, Tiwari AK, Raman D. Targeting of the Eukaryotic Translation Initiation Factor 4A Against Breast Cancer Stemness. Front Oncol. 2019;9:1311.
24. Ravazoula P, Batistatou A, Aletra C, Ladopoulos J, Kourounis G, Tzigounis B. Immunohistochemical expression of glucose transporter Glut1 and cyclin D1 in breast carcinomas with negative lymph nodes. Eur J Gynaecol Oncol. 2003;24(6):544–6.
25. Targeting Hypoxia-Inducible Factor. -1 alpha/Pyruvate Dehydrogenase Kinase 1 Axis by Dichloroacetate Suppresses Bleomycin-induced Pulmonary Fibrosis %J. American journal of respiratory cell molecular biology. 2018;58(2):216–31.
26. Wan J, Chai H, Yu Z, Ge W, Kang N, Xia W, Che Y. HIF-1alpha effects on angiogenic potential in human small cell lung carcinoma. J Exp Clin Cancer Res. 2011;30:77.
27. Brustugun T, OJSiro. Hypoxia as a Cause of Treatment Failure in Non-Small Cell Carcinoma of the Lung. 2015,25(2):87–92.
28. Hayashi M, Sakata M, Takeda T, Yamamoto T, Okamoto Y, Sawada K, Kimura A, Minekawa R, Tahara M, Tasaka K, et al. Induction of glucose transporter 1 expression through hypoxia-inducible factor 1alpha under hypoxic conditions in trophoblast-derived cells. J Endocrinol. 2004;183(1):145–54.
29. Zhang TB, Zhao Y, Tong ZX, Guan YF. Inhibition of glucose-transporter 1 (GLUT-1) expression reversed Warburg effect in gastric cancer cell MKN45. Int J Clin Exp Med. 2015;8(2):2423–8.
30. Wohlbold L, Merrick KA, De S, Amat R, Kim JH, Larochelle S, Allen JJ, Zhang C, Shokat KM, Petrini JH, et al. Chemical genetics reveals a specific requirement for Cdk2 activity in the DNA damage response and identifies Nbs1 as a Cdk2 substrate in human cells. PLoS Genet. 2012;8(8):e1002935.

31. Sun K, Leung L, Therapy WJG. Gene transfer of antisense hypoxia inducible factor-1 α enhances the therapeutic efficacy of cancer immunotherapy. 2001,8(8):638–645.
32. Acker T, Plate KH. A role for hypoxia and hypoxia-inducible transcription factors in tumor physiology. J Mol Med (Berl). 2002;80(9):562–75.

Figures

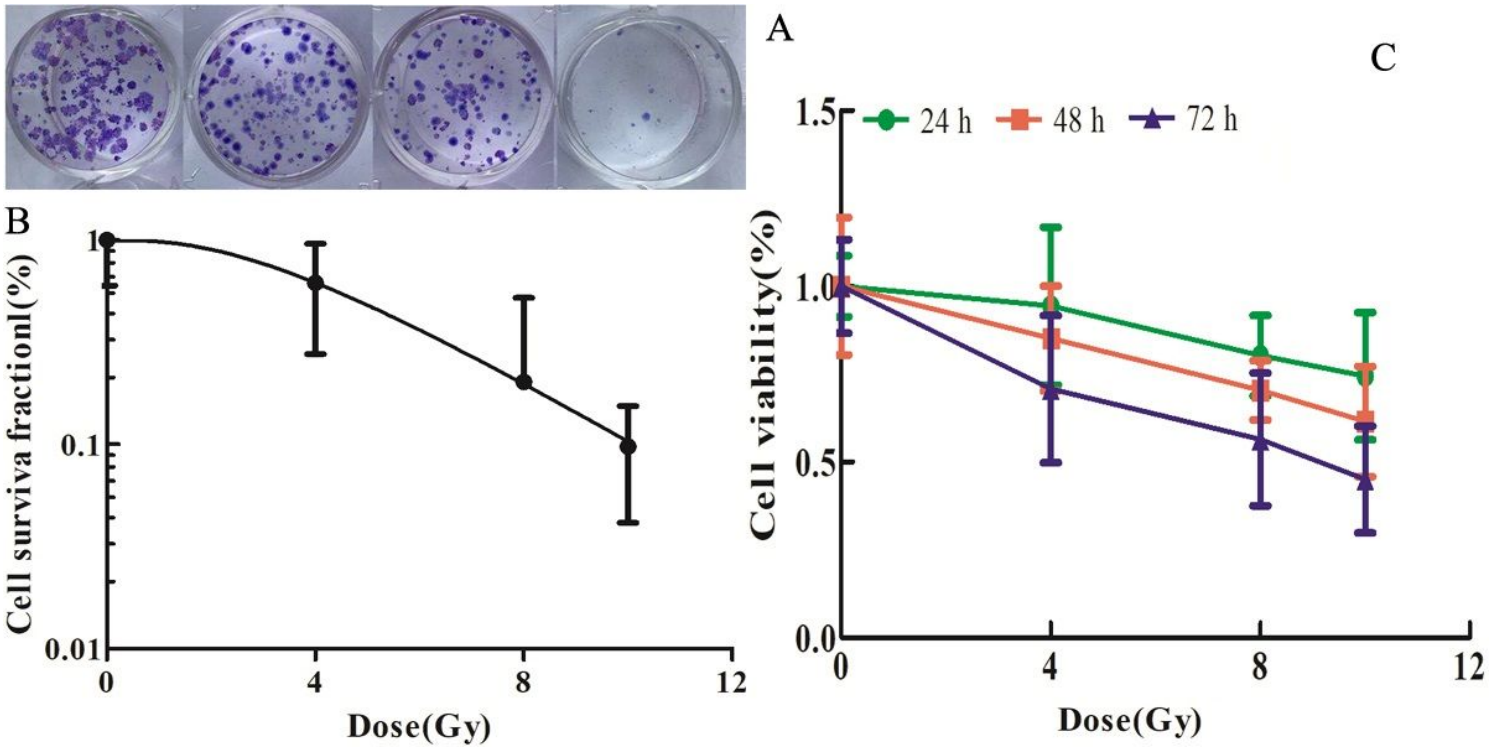

Figure 1

Proliferation inhibition effect of photons on H1299 cells. (A) Radiation-induced cell colony formation. (B) LQ model for ionizing radiation. (C) Inhibitory effect of photon radiation on cell proliferation.

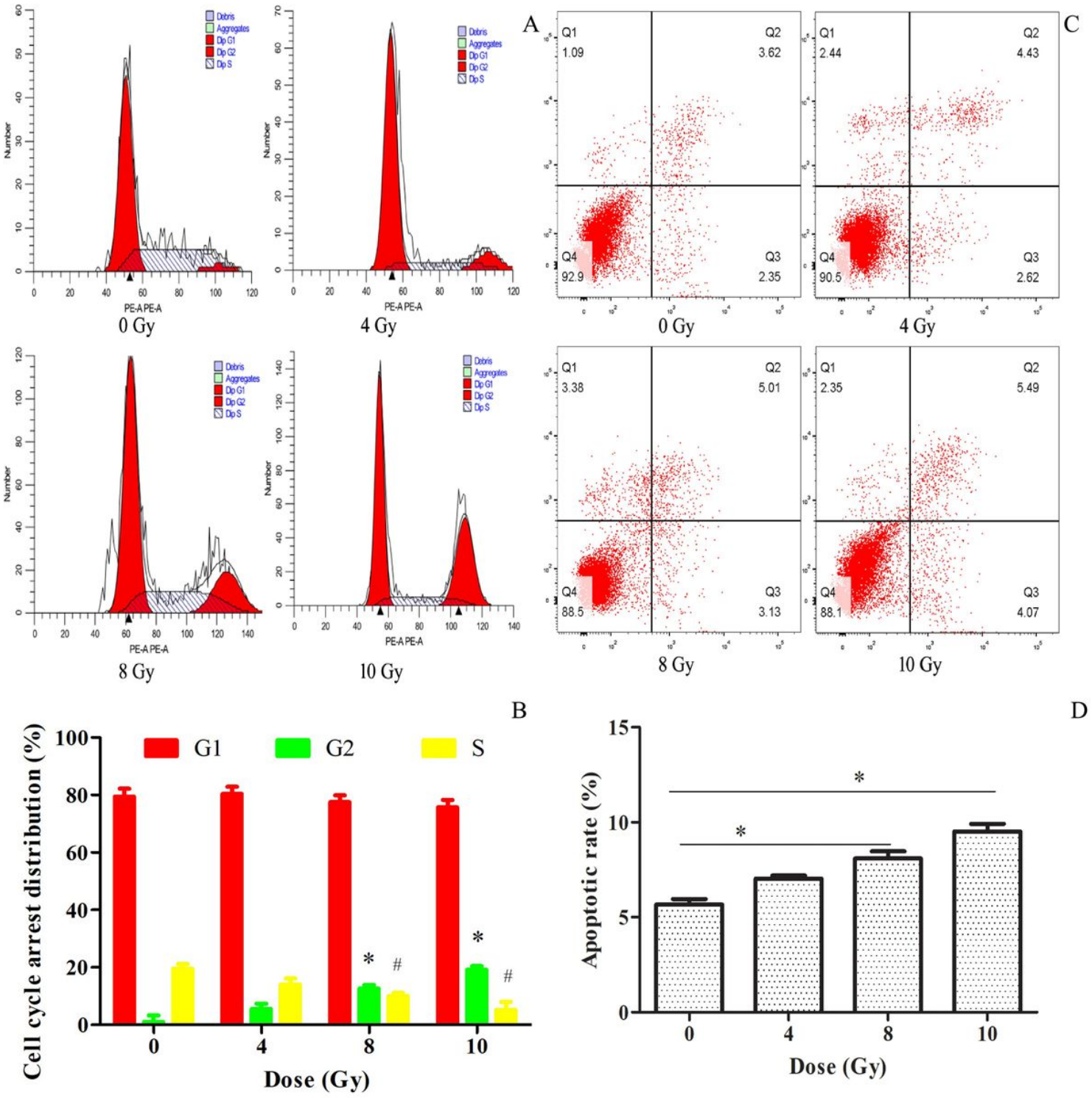

Figure 2

Radiation-induced changes in cell cycle and apoptosis in H1299. (A) Radiation-induced cell cycle distribution. (B) Statistical analysis of cell cycle phases. (C) Radiation-induced changes in apoptosis. (D) Statistical analysis of the percentage of apoptosis. (*P <0.05).

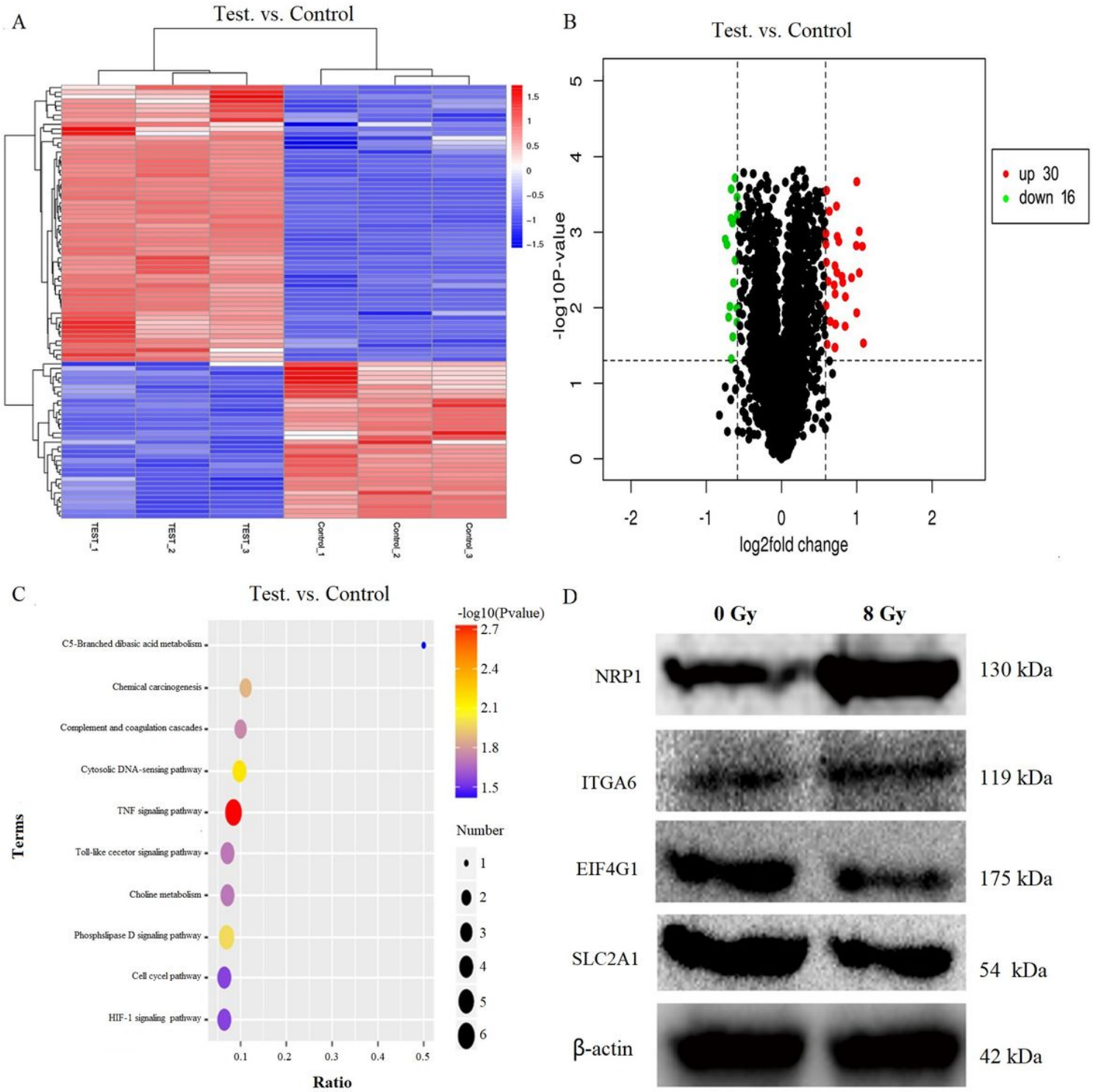

Figure 3

Screening and verification of differential molecules (A) Cluster analysis. (B) Volcano diagram. (C) KEGG signaling pathway.(D) Western blotting analysis.

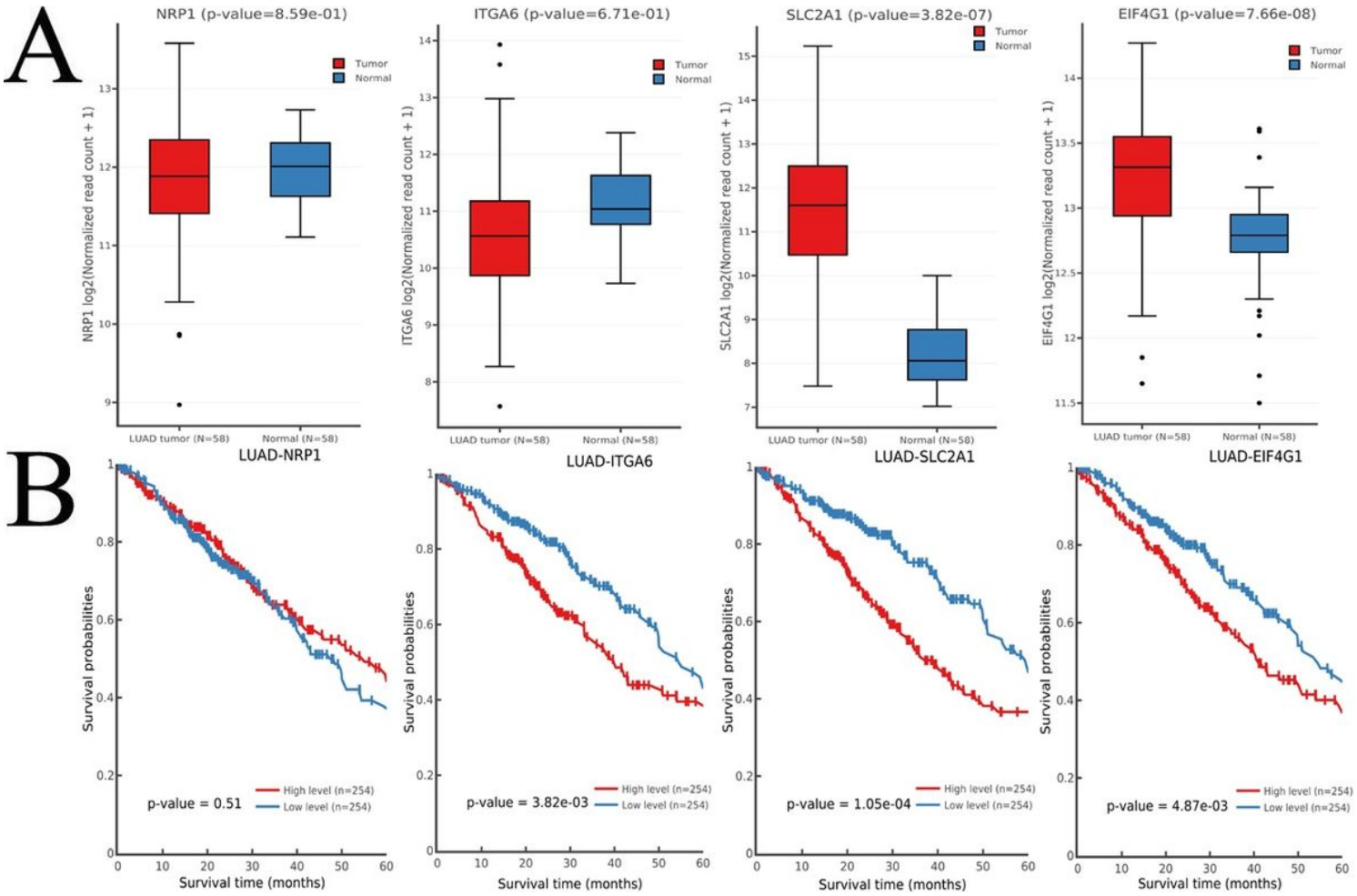

Figure 4

Differential protein expression and survival analysis in lung adenocarcinoma TCGA database. (A) Differential protein expression in tumors and tissues. (B) Differential molecules and five-year survival of cancer patients.

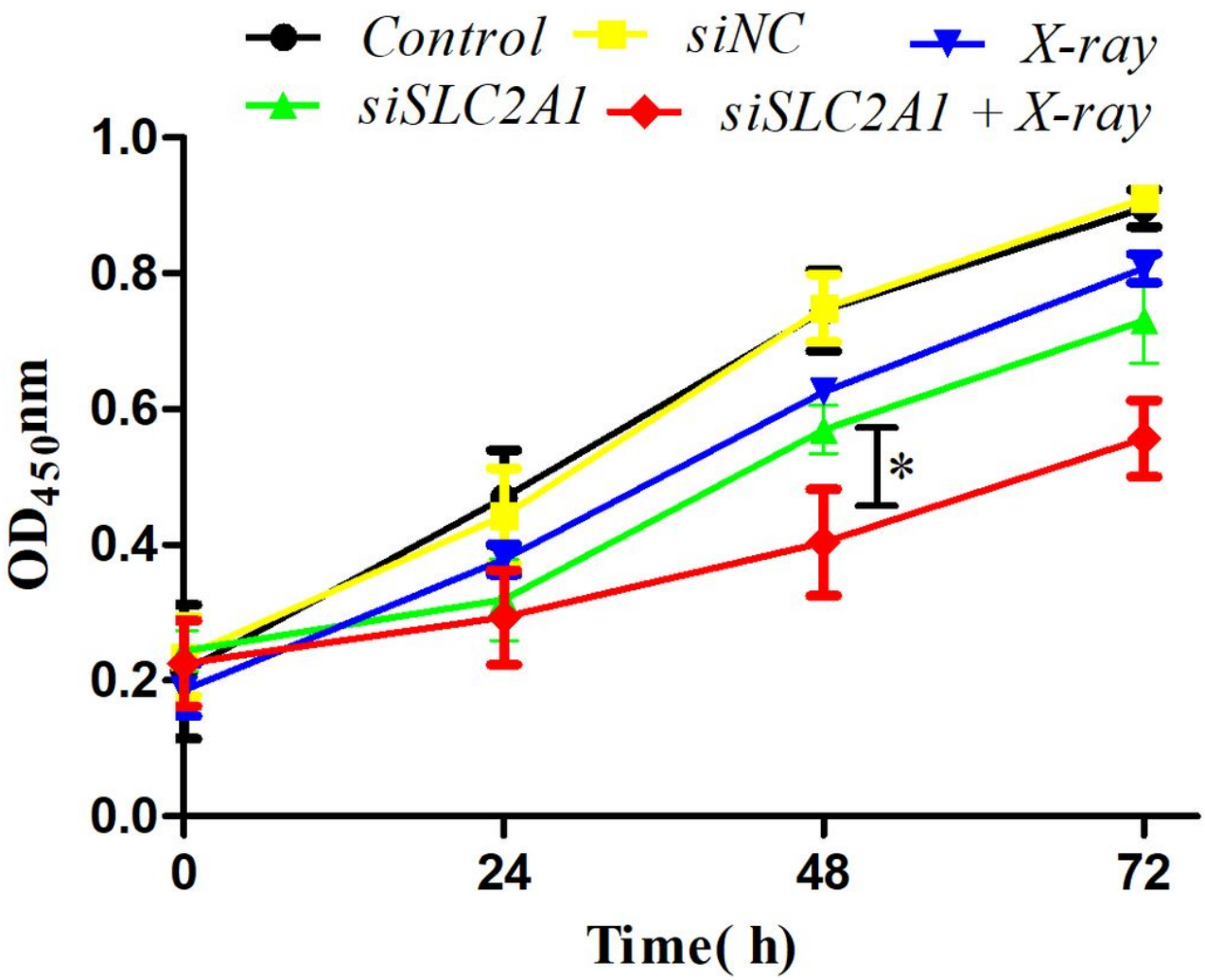

Figure 5

Knockdown SLC2A1 combined with X-ray can inhibit cell proliferation.

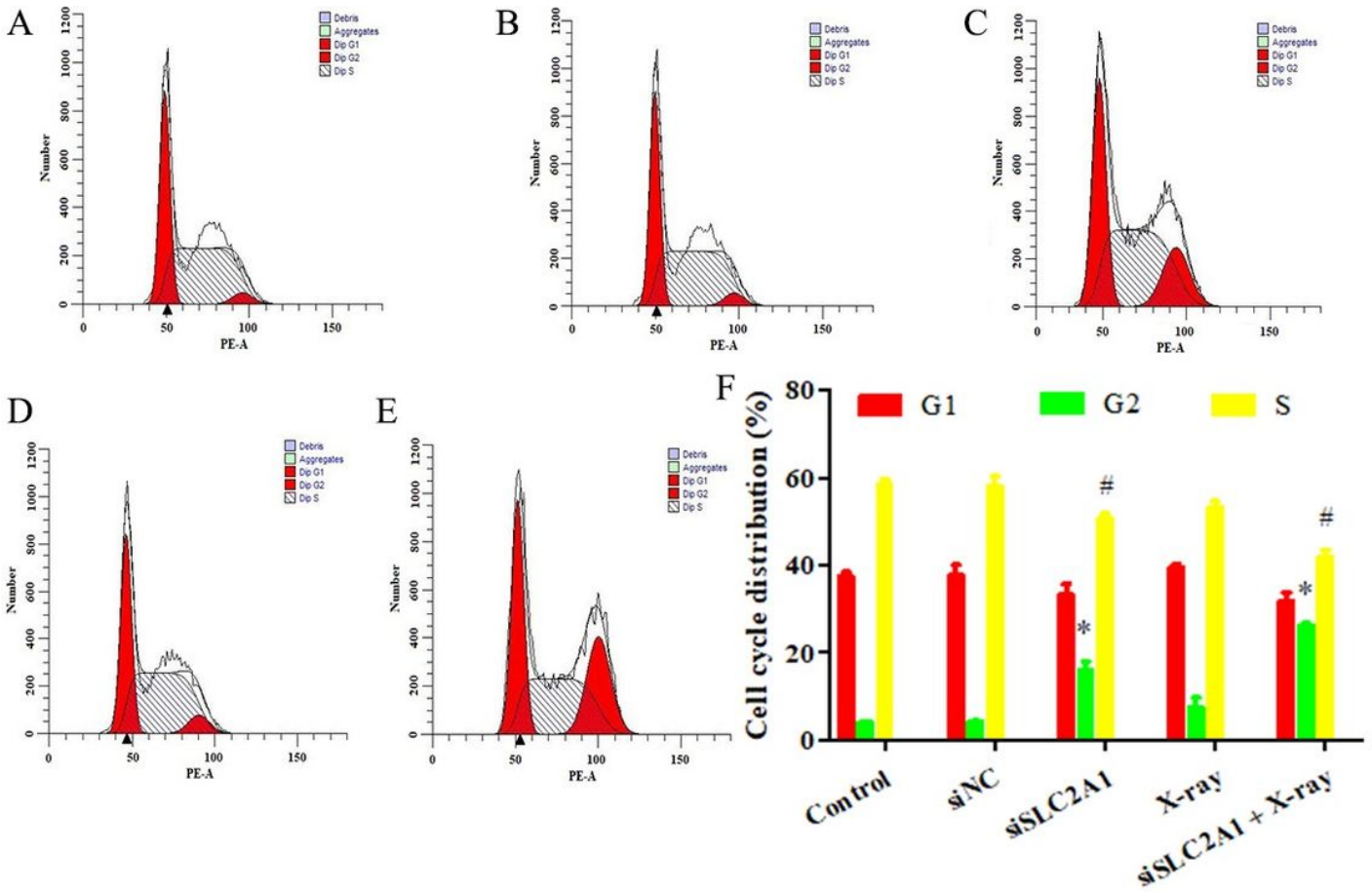

Figure 6

Flow cytometry analysis of cell cycle distribution of H1299 cells after 4Gy radiation under normal and knockdown conditions (*,# $p < 0.05$).

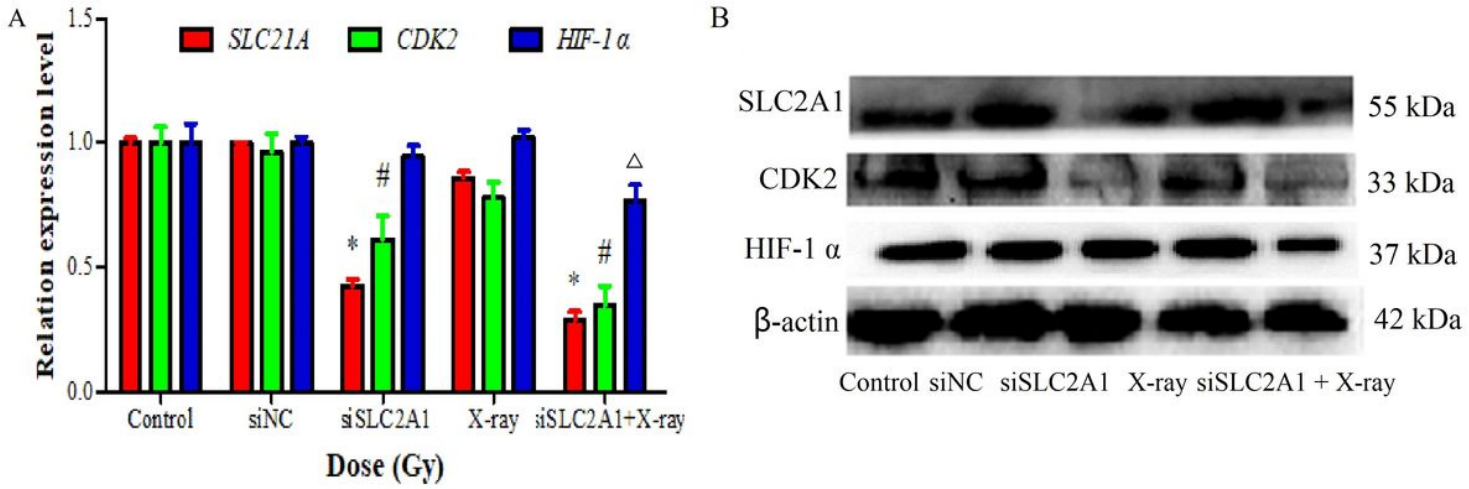

Figure 7

Western blot and RT-PCR of SLC2A1, Cdk2 and HIF-1a expression in H1299 cells irradiated with 4 Gy control and knockdown condition. (A) mRNA expression levels. (B) protein expression levels(*,#,△$p < 0.05$).

Supplementary Files

This is a list of supplementary files associated with this preprint. Click to download.

- Supplementary.rar